M(μ-CN)Fe(μ-CN)M′ Chains with Phthalocyanine Iron Centers: Preparation, Structures, and Isomerization

Andreas Geiss and Heinrich Vahrenkamp*

Institut für Anorganische und Analytische Chemie der Universität Freiburg, Albertstrasse 21, D-79104 Freiburg, Germany

Received January 31, 2000

The molecular building blocks Fe(II)Pc (Pc = phthalocyaninato^{2-}), Fe(III)Pc, ZnPc, Cp(dppe)Fe, and Cp(PPh_3)$_2$Ru were combined in the cyanide-bridged dinuclear reference compounds with M−CN−ZnPc and M−CN−FePc−CN arrays containing Fe(II)Pc and Fe(III)Pc. The linear trinuclear species with the M(μ-CN)Fe(μ-CN)M′ backbone were prepared for both Fe(II)Pc and Fe(III)Pc centers, for terminal Fe/Fe, Fe/Ru, and Ru/Ru combinations and for all three possible cyanide orientations (M−CN−Fe−NC−M′, M−CN−Fe−CN−M′, and M−NC−Fe−CN−M′). The 15 complexes obtained were identified from their IR spectra and six structure determinations. The preferred orientation of the cyanide bridges could be established starting from the [Fe−NC−Fe(III)Pc−CN−Fe]$^+$ complex, which is labile in solution and isomerizes to the corresponding [Fe−CN−Fe(III)Pc−NC−Fe]$^+$ complex. A kinetic analysis of this isomerization has yielded an activation barrier of roughly 110 kJ/mol.

Compounds with $M_x(CN)_y$ arrays play a dominant role in the study of new materials comprised of covalently linked one-, two-, or three-dimensional structures. Several recent reviews[1−5] have emphasized the value of polymeric cyanometallics in electrical conductance, energy conversion, or phenomena related to color or magnetism. The basis for all this is the ability of bridging cyanide ligands to mediate electronic communication between metal atoms, i.e., electron transfer, mixed-valence, or magnetic interactions.[6−13]

To gain an understanding of this basic phenomenon, molecular compounds with chainlike arrangements of metal atoms and bridging cyanide ligands should be useful. Quite a number of such compounds have been described and subjected to physical investigation.[13] During these studies, it was found, however, that the construction of $(M-CN)_n$ chains with more than two metal atoms is challenging, and despite some reports on oligonuclear chainlike complexes,[14,15] no such species with more than three metal atoms has been fully characterized until now.

We have set out to improve the synthetic accessibility of such species and to systematize their metal−metal charge-transfer properties along the way. After some basic investigation on dinuclear systems,[16] we have elaborated for trinuclear complexes the effects of the geometry at the central metal (cis- or trans-octahedral, trans-square planar, and tetrahedral) and of the orientation of the cyanide bridges (M−CN−M′ vs M−NC−M′) on the electronic communication between the two external metals.[17−20] Tetranuclear complexes with two cyanide bridges[21] as well as polynuclear species with a central Fe_4S_4 core[22] were found to exhibit quite a variation of metal−metal interactions.

It seemed to us that the redox activity at the central metal units might be influential on these variations. With this in mind, we started the work reported in this paper. A central metal complex unit capable of multiple one-electron transfers was chosen to be cyanide-linked to two external metal complex units susceptible to single-electron transfer. The easily available phthalocyanine iron unit, whose redox properties are well-investigated and which ensures that the two external cyanometal units are favorably (i.e., trans) oriented, was chosen as the center. The external metal units were those we had found most favorable for this purpose,[17−19] namely, the electron-rich Cp(dppe)Fe and Cp(PPh_3)$_2$Ru units. This paper describes the syntheses, structures, IR spectra, and isomerization of the trinuclear complexes. The accompanying paper[23] dwells on their electronic situations before and after single-electron redox processes.

Results and Discussion

Starting Materials. The central building blocks of all complexes were the phthalocyaninato−metal units MPc with M = Fe(II), Fe(III), or Zn(II). They were used, for example, as

(1) Fehlhammer, W. P.; Fritz, M. *Chem. Rev.* **1993**, *93*, 1243.
(2) Kahn, O. *Adv. Inorg. Chem.* **1995**, *43*, 179.
(3) Balzani, V.; Juris, A.; Venturi, M.; Campagna, S.; Serroni, S. *Chem. Rev.* **1996**, *96*, 759.
(4) Dunbar, K. R.; Heintz, R. A. *Prog. Inorg. Chem.* **1997**, *45*, 283.
(5) Bignozzi, C. A.; Schoonover, J. R.; Scandola, F. *Prog. Inorg. Chem.* **1997**, *44*, 1.
(6) Robin, M. D.; Day, P. *Adv. Inorg. Chem. Radiochem.* **1967**, *10*, 247.
(7) Taube, H. *Electron Transfer Reactions of Complex Ions in Solution*; Academic Press: New York, 1970.
(8) Creutz, C. *Prog. Inorg. Chem.* **1983**, *30*, 1.
(9) Vogler, A.; Osman, A. H.; Kunkely, H. *Coord. Chem. Rev.* **1985**, *64*, 159.
(10) Kalyanasundaram, K.; Nazeeruddin, M. K. *Inorg. Chim. Acta* **1994**, *226*, 213.
(11) Coe, B. J.; Meyer, T. J.; White, P. S. *Inorg. Chem.* **1995**, *34*, 3600.
(12) Connelly, N. G.; Lewis, G. R.; Moreno, M. T.; Orpen, A. G. *J. Chem. Soc., Dalton Trans.* **1998**, 1905.
(13) Vahrenkamp, H.; Geiss, A.; Richardson, G. N. *J. Chem. Soc., Dalton Trans.* **1997**, 3643, and references therein.
(14) Argazzi, R.; Bignozzi, C. A.; Garcia, C. G.; Meyer, T. J.; Scandola, F.; Schoonover, J. R. *J. Am. Chem. Soc.* **1992**, *114*, 8727.
(15) Chang, C.; Ludwig, D.; Bocarsly, A. *Inorg. Chem.* **1998**, *37*, 5467.
(16) Zhu, N.; Vahrenkamp, H. *Chem. Ber.* **1997**, *130*, 1241.
(17) Zhu, N.; Vahrenkamp, H. *J. Organomet. Chem.* **1990**, *573*, 67.
(18) Richardson, G. N.; Brand, U.; Vahrenkamp, H. *Inorg. Chem.* **1999**, *38*, 3070.
(19) Geiss, A.; Vahrenkamp, H. *Eur. J. Inorg. Chem.* **1999**, 1793.
(20) Richardson, G. N.; Vahrenkamp, H. *J. Organomet. Chem.* **2000**, *593*−*594*, 44.
(21) Geiss, A.; Keller, M.; Vahrenkamp, H. *J. Organomet. Chem.* **1997**, *541*, 441.
(22) Zhu, N.; Appelt, R.; Vahrenkamp, H. *J. Organomet. Chem.* **1998**, *565*, 187.
(23) Geiss, A.; Kolm, M. J.; Janiak, C.; Vahrenkamp, H. *Inorg. Chem.*, **2000**, *39*, 4037−4043.

10.1021/ic0001412 CCC: $19.00
Published on Web 08/11/2000

Fe(II)Pc and Zn(II)Pc. The simplest Fe(III) derivative used was Fe(III)PcCl. Both Fe(II) and Fe(III) were also introduced as the cyano complexes $[Fe(II)Pc(CN)_2]^{2-}$ and $[Fe(III)Pc(CN)_2]^-$ with PPN counterions. The terminal electron-rich organometallic units containing Fe(II) or Ru(II) were attached starting from the halides **1a** and **2a** or from the cyanides **1b** and **2b**.

$Cp(dppe)Fe-Br$	$Cp(PPh_3)_2Ru-Cl$
1a	**2a**
$Cp(dppe)Fe-CN$	$Cp(PPh_3)_2Ru-CN$
1b	**2b**

Dinuclear Reference Compounds. To quantify the basic spectroscopic, structural, and redox features of the MPc/CN/MCp combinations, we prepared some dinuclear species, i.e., those with only one MCp per MPc unit. The simplest of these, having only one redox-active metal center, are **3** and **4**. These uncharged complexes were obtained by simple combination of the uncharged ZnPc constituents and **1b** or **2b**. The other two dinuclear complexes **5** and **6** contain two redox-active metal centers as well as one bridging and one nonbridging cyanide ligand. They were prepared by the substitution of one cyanide ligand in $[Fe(III)Pc(CN)_2]^-$ with the ligand **1b** or **2b**.

M−CN−ZnPc:
3, M = Cp(dppe)Fe; **4**, M = $Cp(PPh_3)_2Ru$

M−CN−Fe(III)Pc−CN:
5, M = Cp(dppe)Fe; **6**, M = $Cp(PPh_3)_2Ru$

The IR data of the dinuclear complexes, which are listed in Table 1, together with reference values, confirm some basic features of cyanide bridging.[18,19] The kinematic effect—i.e., the constraint of the C−N vibration due to metal attachment at both C and N—increases $\tilde{\nu}$(CN) in comparison to the ligands **1b** and **2b**. Overcompensation for this by increased back-bonding at the C terminus (which, in turn, is induced by strongly electron-accepting metals at the N terminus) is not observed: in all four dinuclear complexes, $\tilde{\nu}$(CN) of the ligands **1b** and **2b** is increased by ca. 10 cm^{-1}. This leads to the conclusion that ZnPc and Fe(III)Pc in these systems have similar electron-pair-acceptor qualities. Complexes **5** and **6** display a second CN band at higher wavenumbers, which is assigned to the Fe(III)-bound terminal cyanide. It is of higher wavenumber because the electron-poor Fe(III)Pc provides much less π-back-donation to the CN carbon than the very electron-rich bis(phosphine)MCp units. At the same time, this band at ca. 2125 cm^{-1} provides a rough estimate of the CN band position in $[Fe(III)Pc(CN)_2]^-$, in which the CN band is so weak that it remains unobserved.[24]

Table 1. IR Data[a] for Mono- and Dinuclear Complexes

complex	$\tilde{\nu}$(CN)
1b	2062m
2b	2072m
3	2070m
4	2082m
5	2124w, 2071s
6	2125w, 2083s

[a] Samples dissolved in CH_2Cl_2, $\tilde{\nu}$ reported in cm^{-1}.

Two of the dinuclear complexes were characterized by structure determinations. Among all the MPc complexes described here, the zinc complexes **3** and **4** are the only ones without an octahedrally coordinated metal ion in the center of the phthalocyanine ring. The structure of **3** (Figure 1) visualizes this. Like in other PcZn−X complexes,[25,26] the metal is lifted by about 0.5 Å out of the Pc ligand, which itself is no longer planar but bent away from the zinc ion. Bond lengths and angles at both zinc[25,26] and iron[16−19] are in the normal range. The bridging cyanide ligand shows a typical bending feature: while the Fe−C−N sequence (173°) is reasonably close linear, the Zn−N−C sequence (150°) is severely bent, in accordance with the lack of any π-interaction between zinc and the N terminus of CN. As observed many times before,[16−19] this is the simplest way to identify the C and N termini of the bridging cyanide, which are basically indistinguishable by crystallographic means alone.

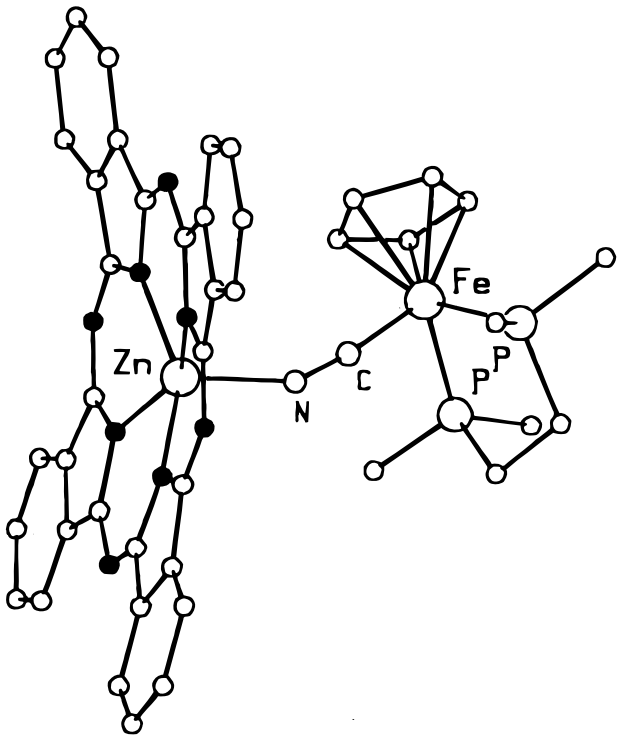

Figure 1. Molecular structure of **3** (phenyl groups at phosphorus omitted for clarity). Important bond lengths and angles: Zn−N(Pc), 2.042−2.061(3) Å; Zn−N(CN), 2.039(3) Å; Fe−P, 2.181(1) and 2.185(1) Å; Fe−C(CN), 1.856(4) Å; C−N, 1.162(5) Å; Zn−N−C, 150.2(3)°; Fe−C−N, 172.8(3)°.

Complex **6** (Figure 2) contains octahedral Fe(III) located roughly in the plane of the four Pc nitrogens and bearing one C-bound and one N-bound cyanide. The Pc ligand is distinctly nonplanar. Its saddle shape is expressed by the interplanar angles between the FeN_4 plane and the planes of its phenyl rings, which range between +14°and −7°. The features of the $Cp(PPh_3)_2Ru$ unit[16−19] are again normal. The orientations of the two cyanide ligands are as expected from the synthesis. Their distinction rests again on the stronger bending of the Fe−N−C sequence (163°) compared to that of the Fe−C−N sequence (178°). In contrast, the small difference of the Fe−C(CN) and Fe−N(CN) bond lengths (1.950 vs 1.975 Å) would not allow the distinction. It should be noted, however, that π-back-donation has made the Fe−C(CN) distance shorter than the Fe−N(CN) distance, contrary to the smaller radius of N. As usual, the small difference of the C−N bond lengths (1.15 vs 1.14 Å) does not reflect their completely different bonding modes.

(24) Kalz, W.; Homborg, H.; Küppers, H.; Kennedy, B. J.; Murray, K. S. *Z. Naturforsch.* **1984**, *39b*, 1478.
(25) Assmann, B.; Sievertsen, S.; Homborg, H. *Acta Crystallogr., Sect. C* **1996**, *52*, 876.
(26) Kobayashi, T.; Ashida, T.; Uyeda, N.; Suito, E.; Kakudo, M. *Bull. Chem. Soc. Jpn.* **1971**, *44*, 2095.

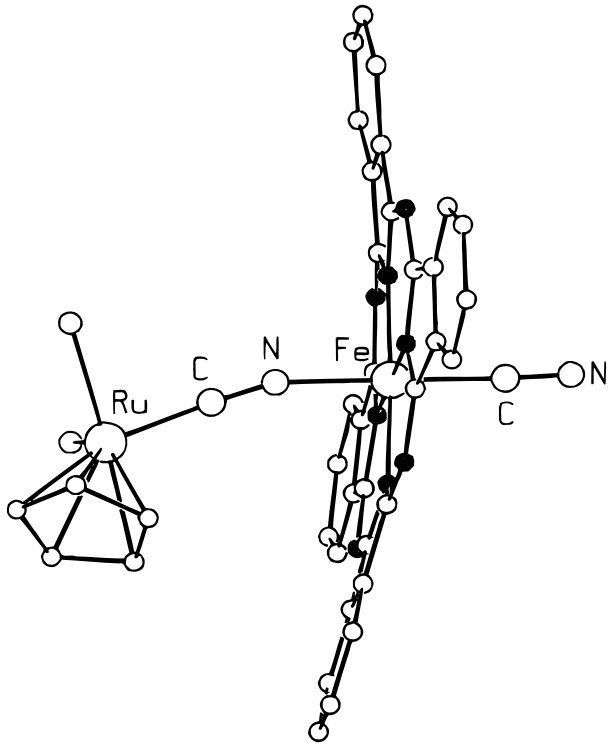

Figure 2. . Molecular structure of **6** (phenyl groups at phosphorus omitted for clarity). Important bond lengths and angles: Fe−N(Pc), 1.945−1.956(7) Å; Fe−N(CN), 1.975(6) Å; Fe−C(CN), 1.950(8) Å; C−N(Fe−C), 1.14(1) Å; C−N(Fe−N), 1.15(1) Å; Ru−C(CN), 1.977(8) Å; Ru−P, 2.309(2) and 2.309(2) Å; Fe−N−C, 163.4(7)°; Fe−C−N, 177.7(8)°; Ru−C−N, 175.1(7)°.

Syntheses of Trinuclear Complexes. All trinuclear complexes decribed here are based on central FePc units. In the M(μ-CN)FePc(μ-CN)M arrays, three orientations of the bridging cyanide ligands are possible. Their annotation as **a**, **b**, and **c** is shown below. Examples for all three orientations were obtained. We found five cases where two of the isomers could be isolated, and in one case, the third isomer could also be obtained. Furthermore, the stability of the FePc unit for both Fe(II) and Fe(III) has allowed us to prepare pairs of trinuclear complexes which differ only in the oxidation state of the central iron atom. We have isolated three pairs of such complexes.

M−CN−Fe−NC−M
a

M−CN−Fe−CN−M
b

M−NC−Fe−CN−M
c

The simplest preparation, the direct attachment of two cyanometal ligands to an FePc unit, worked for Fe(II)Pc and both ligands **1b** and **2b** and yielded the expected symmetrical trinuclear complexes **7a** and **8a**. As shown below (and in the accompanying paper),[23] isomer **a** with the nitrogen termini of both bridging cyanides attached to the central FePc unit is thermodynamically preferred. This seems to be the reason why attempts were almost futile in preparing isomers **7c** and **8c** with the inverse orientation of both cyanides. Reactions of $[Fe(II)Pc(CN)_2]^{2-}$ with **1a** invariably produced mixtures of **7a** and **7c**, and only in one case could a reasonably pure fraction of **7c** be isolated (the purity of which was ascertained by cyclic voltammetry).[23] When $[Fe(II)Pc(CN)_2]^{2-}$ was treated with **2a,** the reaction took yet another course: only one CN ligand was reoriented, and the asymmetrical isomer **8b** was the only product formed. The isomers **a**, **b**, and **c** differ insignificantly in their NMR spectra (see Experimental Section), but the combination of their IR (see below), electrochemical,[23] and UV−Vis−NIR investigation[23] did make their assignments unambiguous.

M−CN−Fe(II)Pc−NC−M:
7a, M = Cp(dppe)Fe; **8a**, M = $Cp(PPh_3)_2Ru$

Cp(dppe)Fe−NC−Fe(II)Pc−CN−Fe(dppe)Cp
7c

$Cp(PPh_3)_2Ru$−CN−Fe(II)Pc−CN−$Ru(PPh_3)_2Cp$
8b

Several approaches were used in preparing the trinuclear complexes with central Fe(III)Pc units. The simplest of these started again with the central unit itself, this time as Fe(III)PcCl. Its treatment with **1b** and **2b** yielded, as expected, the thermodynamically preferred isomers **9a** and **10a**, which were isolated as SbF_6 salts. Attempts to prepare their symmetrical isomers **9c** and **10c** from $[Fe(III)Pc(CN)_2]^-$ failed. Treatment of $[Fe(III)Pc(CN)_2]^-$ with **1a** produced **9a** again, i.e., accompanied by reorientation of both CN units. Treatment with **2a** resulted in the formation of the asymmetrical isomer **10b**, i.e., accompanied by reorientation of one CN unit, as observed above in the formation of **8b**.

The formation of **10b** could be independently verified by using the dinuclear complex **6** with one terminal CN ligand as the starting material and reacting it with $[Cp(PPh_3)_2Ru(CH_3CN)]SbF_6$. Likewise, treatment of **5** with **1a** produced the asymmetrical isomer **9b**, which, however, could only be characterized spectroscopically in solution. After workup, only its isomerization product **9a** was isolated. The dinuclear species **5** and **6** could also be used in preparing heterotrinuclear complexes. From **5** and **2a** resulted **11b**; from **6** and **1a** resulted **12b**. Unlike the labile product **9b**, the ruthenium-containing homologues **10b**, **11b**, and **12b** show no tendency to rearrange to their symmetrical isomers **a** at room temperature in solution.

The formation of the third isomer of **9**—namely, **9c**—could finally be achieved by a redox reaction, which, unlike the substitution reactions, can be performed at very low temperatures. Treating the Fe(II) derivative **7c** with $[FeCp_2]SbF_6$ and keeping the temperature below −30 °C during all steps of the procedure allowed the isolation of **9c**. However, when **9c** is dissolved, e.g., for measurements at room temperature, its rearrangement via **9b** to **9a** begins, which is the reason all measurements of **9c** show the presence of **9a**, the amount of which increases with time.

$[M−CN−Fe(III)Pc−NC−M]^+$:
9a, M = Cp(dppe)Fe; **10a**, M = $Cp(PPh_3)_2Ru$

$[M−CN−Fe(III)Pc−CN−M]^+$:
9b, M = Cp(dppe)Fe; **10b**, M = $Cp(PPh_3)_2Ru$

$[M−NC−Fe(III)Pc−CN−M]^+$:
9c, M = Cp(dppe)Fe

$[Cp(dppe)Fe−CN−Fe(III)Pc−CN−Ru(PPh_3)_2Cp]^+$
11b

$[Cp(PPh_3)_2Ru−CN−Fe(III)Pc−CN−Fe(dppe)Cp]^+$
12b

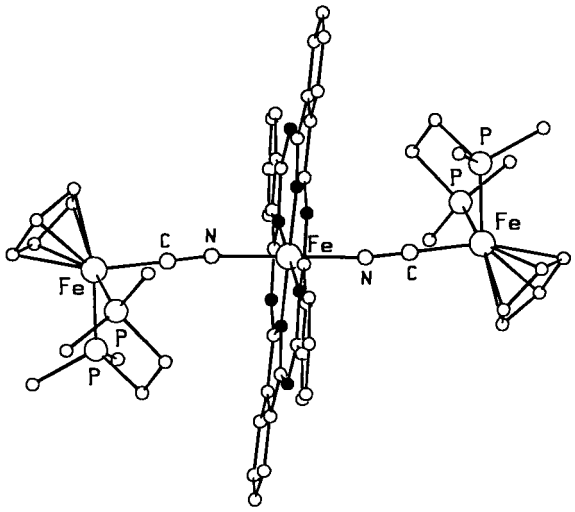

Figure 3. Structure of the trinuclear cation in [**9a**]SbF_6 (phenyl groups at phosphorus omitted for clarity). Important bond lengths and angles: Fe−N(Pc), 1.949(5) and 1.951(5) Å; Fe−N(CN), 1.960(5) Å; Fe−C(CN), 1.888(7) Å; C−N, 1.151(8) Å; Fe−N−C, 172.2(5)°; Fe−C−N, 179.6(6)°.

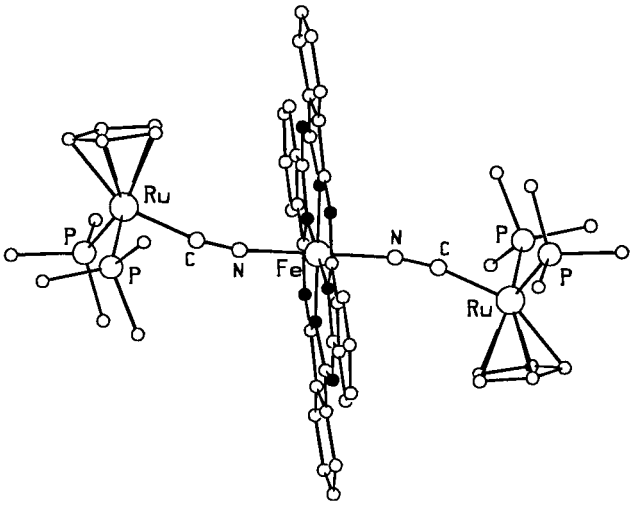

Figure 5. Molecular structure of **8b** (phenyl groups at phosphorus omitted for clarity). Important bond lengths and angles: Fe−N(Pc), 1.929(5) and 1.941(5) Å; Fe−N(CN) and Fe−C(CN), 1.981(5) Å; C−N, 1.130(6) Å; Fe−C−N and Fe−N−C, 169.5(5)°; Ru−N−C and Ru−C−N, 168.6(5)°.

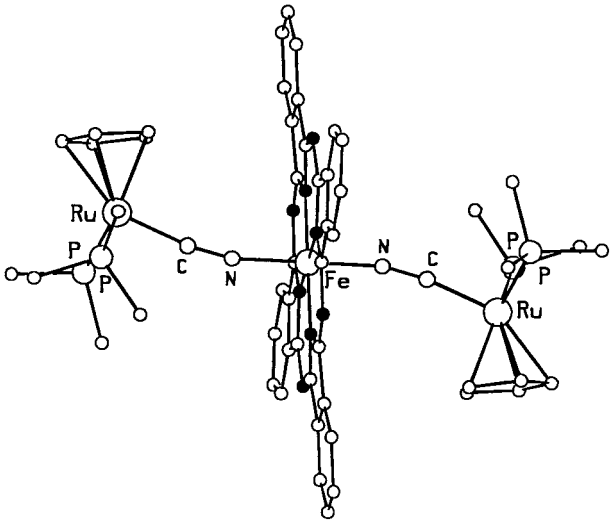

Figure 4. Structure of one of the two trinuclear cations in [**10a**]SbF_6 (phenyl groups at phosphorus omitted for clarity). Important bond lengths and angles: Fe−N(Pc), 1.954(7) and 1.943(6) Å; Fe−N(CN), 1.902(6) Å; Ru−C(CN), 1.953(8) Å; C−N, 1.163(9) Å; Fe−N−C, 166.7(6)°; Ru−C−N, 170.9(6)°.

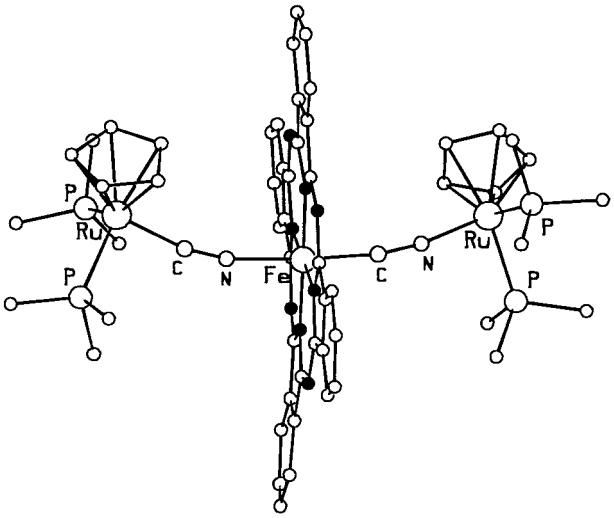

Figure 6. Structure of the trinuclear cation in [**10b**]SbF_6 (phenyl groups at phosphorus omitted for clarity). Important bond lengths and angles: Fe−N(Pc), 1.931(4)−1.948(4) Å; Fe−N(CN), 1.937(5) Å; Fe−C(CN), 1.967(5) Å; Ru−C(CN), 2.022(5) Å; Ru−N(CN), 2.019(5) Å; C−N, 1.133(7) and 1.156(7) Å; Fe−C−N, 166.1(4)°; Fe−N−C, 168.7(4)°; Ru−N−C, 167.6(4)°; Ru−C−N, 168.1(4)°.

Structure of the Trinuclear Complexes. Two pairs of related complexes were chosen for the structure determinations, the Fe/Ru homologues **9a** and **10a** and the redox couple **8b** and **10b**. They will also be discussed as pairs. In all four cases, the external Cp(dppe)Fe and $Cp(PPh_3)_2Ru$ units show no peculiarities in their bond lengths and angles (see above and in refs 16−19) and, hence, will not be discussed here. This holds even for the case of **10a**, which has two independent complex cations in the unit cell differing in their torsion angles around the Fe−NC−Ru axes. The latter, however, does not affect the geometry at the Fe(III) center or the characteristics of the Fe−NC−Ru entities. In all four complexes, the central iron atoms are close to the ideal octahedral coordination, and the phthalocyanine ligands are close to being completely planar.

In both homologues **9a** (Figure 3) and **10a** (Figure 4), the central iron atom occupies an inversion center, and hence, it is surrounded quite symmetrically by the six nitrogen donors. Compared to the Fe(II)Pc complexes **6** and **8b**, there are no significant differences in the Fe−N bond lengths. The orientations of the cyanide ligands can be assigned unambiguously again from the bonding angles at C and N: in both cases, there is a stronger bending at N than at C.

The comparison of the structures of **8b** (Figure 5) and **10b** (Figure 6) offered two valuable pieces of information, i.e., the effects of changing the oxidation state at the central iron atom and the effects of the two different cyanide orientations in the same molecule. It seems, however, that the latter effect is undetectable, as both complexes seem to be disordered in terms of the CN orientations. This is certainly so for **8b**, which has the central Fe(II) on an inversion center. The trinuclear cations of [**10b**]SbF_6 have no inversion symmetry, but the bond lengths and, specifically, the bond angles at the cyanide ligands are so similar that the two Fe(μ-CN)Ru arrays cannot be distinguished. In both cases, it was ascertained with IR spectra after the X-ray measurements that the samples of the structure determinations really contained the asymmetrical **b** isomers.

Complex **10b** can also be compared with its symmetrical isomer **10a**. In **10a**, both the Fe−N(CN) and Ru−C(CN) bond lengths are significantly shorter than their counterparts in (disordered) **10b**. This seems to reflect the thermodynamic preference of the **a** isomers for both the π-back-donation from the elctron-rich organometallic unit to the cyanide carbon and the σ-donation from the cyanide nitrogen to the electron-poor Fe(III) center.

The effects of the redox change in the pair **8b** and **10b** are small, as previously observed for the pair of complexes $(PPN)_2$-$[Fe(II)Pc(CN)_2]$[27] and $PPN[Fe(III)Pc(CN)_2]$.[24] They correspond to the expectation, as all metal-to-cyanide bond lengths in the oxidized species **10b** are sligthly shorter than those in the reduced species **8b**. Prior to this pair, only two redox couples of cyanide-bridged complexes were structurally compared. The couple $[Cp(dppe)Fe-NC-Cr(CO)_5]^0$ and $[Cp(dppe)Fe-NC-Cr(CO)_5]^{+}$[16] shows significant bond length effects upon a change in the redox state, while the couple $[CO(dppm)_2Mn-CN-Rh(CO)_2Cl]^0$ and $[CO(dppm)_2Mn-CN-Rh(CO)_2Cl]^{+}$[28] shows almost no effects.

IR data and Bonding Considerations. The 11 trinuclear complexes represent only two environments of the cyanide bridge: CN links either two iron atoms or one iron and one ruthenium atom. Thus, the kinematic effect, which is influential for IR data but difficult to quantify, can be considered roughly constant for the two environments, and the effects of σ-donation from the N terminus and π-back-donation to the C terminus may be evaluated from the $\tilde{\nu}$(CN) values. Table 2 lists the relevant data. It is noteworthy that the IR bands for the FePc−CN combination with C-bound cyanide are quite weak, with the extreme cases of $[Fe(II)Pc(CN)_2]^{2-}$ (2084 cm^{-1})[27] and $[Fe(III)Pc(CN)_2]^-$ (unobserved,[24] estimated to be near 2125 cm^{-1}; see above).

Table 2. IR Data[a] for Trinuclear Complexes

complex	$\tilde{\nu}$(CN)
7a	2101m
7c	2064vw
8a	2114m
8b	2116m, 2089w
9a	2062s
9b	2053s, 2038m
9c	2034m
10a	2065s
10b	2123m, 2076s
11b	2124w, 2064s
12b	2057m, 2033s

[a] Samples dissolved in CH_2Cl_2, $\tilde{\nu}$ reported in cm^{-1}.

The first and simplest information from the IR data is that the species with a symmetrical cyanide arrangement (**a** and **c** isomers) show only one $\tilde{\nu}$(CN) band, as expected. The **b** isomers, which are asymmetrical with respect to the cyanide or metal arrangement, show two bands.

After the kinematic effect is taken into account, the two effects controlling the ν(CN) frequencies are σ-donation from the N terminus (which increases $\tilde{\nu}$) and π-back-donation to the C terminus (which decreases $\tilde{\nu}$).[13] It is our experience[16−19] that the presence of a strong σ-acceptor at the N terminus can induce so much π-back-donation at the C terminus that the expected increase in $\tilde{\nu}$ is overcompensated and a lowering of the CN band position is actually observed. In the present case, there seems to be a balanced situation for the complexes containing Fe(III)Pc in the center. When the $\tilde{\nu}$(CN) value of **1b** (2062 cm^{-1}) is compared with the corresponding values of **5**, **9a**, **9b**, and **11b**, or when the value of **2b** (2072 cm^{-1}) is compared with the values of **6**, **10a**, **10b**, and **12b**, little change is observed. For the complexes containing Fe(II)Pc in the center, the situation is different: in going from **1b** to **7a** or from **2b** to **8a** or **8b**, the $\tilde{\nu}$(CN) value rises by about 40 cm^{-1}. The explanation for this is that Fe(II)Pc is a much weaker σ-acceptor than Fe(III)Pc. It does induce the increase of $\tilde{\nu}$(CN) due to σ-donation, but it does not induce the increase to the extent that excessive π-back-donation from the organometallic unit at the C terminus sets in.

The IR data of the trinuclear complexes also reflect nicely the effects of CN/NC isomerism. With only one exception (**10a**/**10b**), the FePc−NC−M combination produces larger $\tilde{\nu}$(CN) values than the FePc−CN−M combination. In the present case, this seems to indicate that the σ-acceptance is the strongest effect: it is more pronounced for FePc than for the organometallic units.

The best picture of the electronic balancing within the complexes can be obtained by comparing the two components of the redox couples **7a**/**9a**, **8a**/**10a**, and **8b**/**10b**, cf. Table 2. In each case, the $\tilde{\nu}$ value for the FePc−NC unit decreases by 40−50 cm^{-1} upon going from Fe(II)Pc to Fe(III)Pc. The complex pair **8b**/**10b** shows that at the same time, the $\tilde{\nu}$ value for the FePc−CN unit increases by 40 cm^{-1}, indicating significant electronic "motion" along the M(μ-CN)Fe(μ-CN)M chains.

Figure 7 is meant to visualize this electronic motion. First, the oxidation of the FePc centers in type **a** increases the σ-donation from the cyanide nitrogen so much that the overcompensating phenomenon (highly increased back-donation to the cyanide carbon) occurs and $\tilde{\nu}$(CN) sinks. Second, the oxidation of the FePc center in type **b** significantly reduces its π-back-donation ability while the σ-accepting ability of the N-bound Ru unit remains the same, and hence, $\tilde{\nu}$ for the FePc−CN unit increases. This mutual compensation of increasing and decreasing $\tilde{\nu}$(CN) seems to occur only for the M−CN−FePc−CN−M arrays: a comparison of **7c** and **9c** shows that yet another type of compensation leads to a decrease in $\tilde{\nu}$ for the FePc−CN units upon oxidation. Altogether, the electronic mobility across the CN bridges in these compounds provides a preview of their metal−metal charge-transfer properties, which are discussed in the accompanying paper.[23]

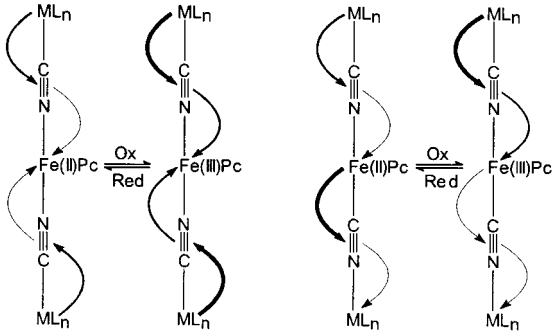

Figure 7. Schematic representation of the donator−acceptor interactions in the trinuclear complexes of type **a** (left) and **b** (right) and their variation upon oxidation and reduction.

Isomerization of Complex 9. As observed during the syntheses of the trinuclear complexes and as previously discussed, the isomers containing cyanide N-bound to the central FePc units seem to be thermodynamically preferred. While the CN/NC isomerization was observed during the syntheses of **8b**,

(27) Küppers, H.; Eulert, H. H.; Hesse, K. F.; Kalz, W.; Homborg, H. *Z. Naturforsch.* **1986**, *41b*, 44.

9a, and **10b**, only one such system was found to show isomerization in solution after its preparation: both complexes **9b** and **9c** are slowly converted to **9a**, which also means that they could not be obtained free of their isomerization products.

To gain quantitative information on the isomerizations, we subjected them to a kinetic treatment. For this purpose, freshly prepared solutions of **9b** (from **5** and [Cp(dppe)Fe(CH_3CN)]SbF_6) and **9c** (from **7c** and [$FeCp_2$]SbF_6) in dichloromethane were placed in a NIR spectrometer, and their spectra were recorded continuously in the 750−2500 nm range (where the characteristic NIR absorptions of **9a** (1295 nm), **9b** (1300 and 2150 nm) and **9c** (2250 nm) are located; see acompanying paper).[23] The spectral traces with perfect isosbestic points in Figure 8 show that the isomerizations are clean and lead only to **9a**.

The quantitative analysis of the **9b** → **9a** interconversion was found to be difficult, probably because the rate of the formation of **9b** from **5** and the rate of isomerization are not too different. The **9c** → **9a** interconversion could be subjected to an approximate kinetic analysis, but the kinetic curves (I_o/I vs time at varying temperatures, cf. figures in the Supporting Information) are sigmoidal and, hence, do not support a clean first-order process. Thus, all kinetic data derived from them have to be considered with caution.

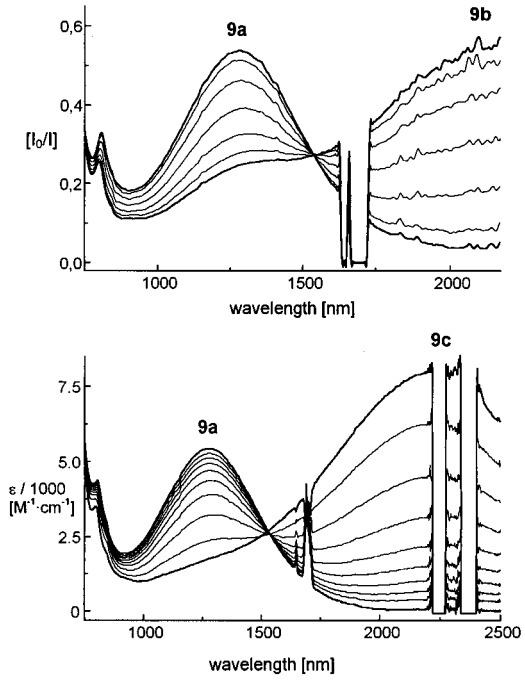

Figure 8. NIR spectra of 10^{-3} M solutions of **9b** (top) and **9c** (bottom) at room temperature in CH_2Cl_2 at 30 min intervals showing their isomerization to **9a**. The breakdowns in the spectral traces are artifacts caused by the spectrometer.

An estimate of the activation barrier of the cyanide/isocyanide isomerization **9c** → **9a** was obtained as follows: the linear sections of the log plots (ln A vs time with $A(t)$ = abs(max) − abs(t), linear after approximately one-fourth of the total reaction time, cf. figures in the Supporting Information) were taken as measures of a monomolecular reaction and used to obtain the first-order rate constants according to $\ln A(t) = -k_n t$. These rate constants are in the range of 1×10^{-4} s^{-1} at 290 K to 7×10^{-3} s^{-1} at 320 K. A log plot ($\ln k_n$ vs $1/T$, cf. figures in the Supporting Information) then yielded the activation energy according to $\ln k_n = \ln k_o - E_a/RT$. Its value is 112 ± 2 kJ/mol. This value cannot be more than a rough estimate, due to the problems mentioned above. In addition, it is by no means obvious that the CN/NC rearrangement is a monomolecular process. Nevertheless, this value is, to our knowledge, the first value of an activation barrier for this process that has been determined.

Conclusions

The application of the appropriate synthetic procedures has made it possible to obtain dinuclear and trinuclear cyanide-bridged complexes with central FePc units which display the following features: (i) redox couples, i.e., the existence of pairs of complexes differing only in the oxidation state of the central iron atom; (ii) cyanide/isocyanide isomerism, i.e., the existence of pairs and triples of complexes differing only in the cyanide arrangement, i.e., CN−Fe−NC vs CN−Fe−CN vs NC−Fe−CN; (iii) metal sequence isomerism, i.e., the existence of complexes with Fe−CN−FePc−CN−Ru and Ru−CN−FePc−CN−Fe arrays. Six structure determinations have revealed gross similarities among the complexes with the unfavorable consequence that complexes with asymmetrical cyanide arrays (e.g., NC−Fe−NC) crystallize in a disordered way; also, in ordered structures, the C and the N of cyanide can be distinguished by the bending of the M−C−N vs M−N−C sequences, which is more pronounced for M−N−C. A comparison of the $\tilde{\nu}$(CN) values of the various isomeric species has allowed the visualization of the transfer of electron density along the M(μ-CN)Fe(μ-CN)M′ chains and its dependency upon the oxidation state of the central iron atom and the varying σ-accepting and π-back-donating abilities of the attached metal−ligand units. This has also allowed us to understand why, among the three complexes with Fe(μ-CN)FePc(μ-CN)Fe arrays, the one with the Fe(II)−CN−Fe(III)Pc−NC−Fe(II) array (i.e., the one occurring in Prussian Blue) is thermodynamically preferred. A preliminary kinetic analysis of the isomerization leading to this array has yielded an estimate of approximately 110 kJ/mol for the activation energy of the cyanide/isocyanide rearrangement, which is the first value reported for such a process.

Experimental Section

The general experimental procedures were as described previously.[16] Fe(II)Pc was obtained commercially. Fe(III)PcCl,[29] PPN[Fe(III)Pc(CN)$_2$],[24] and (PPN)$_2$[Fe(II)Pc(CN)$_2$][27] were prepared as described. The syntheses of the other reagents are listed in ref 16. The NIR spectra were recorded on a Jasco V570 spectrometer.

Complex 3. A solution of ZnPc (220 mg, 0.38 mmol) and **1b** (208 mg, 0.38 mmol) in toluene (100 mL) was heated and refluxed for 5 h. After being filtered, the solution was evaporated to dryness. The residue was taken up in dichloromethane (50 mL), filtered, and layered carefully with petroleum ether (bp 60−70 °C). Within a few days, 156 mg (33%) of **3**·1.5CH_2Cl_2 had separated as dark green crystals (mp 280 °C dec).

Anal. Calcd for $C_{65.5}H_{47}Cl_3FeN_9P_2Zn$ (M_r = 1250.70): C, 62.90; H, 3.87; N, 10.08. Found: C, 62.92; H, 3.91; N, 10.03.

Complex 4. Complex **4** was prepared like complex **3** but with 250 mg (0.43 mmol) of ZnPc and 310 mg (0.43 mmol) of **2b**, yielding 211 mg (38%) of blue-green crystals (mp 265 °C dec).

Anal. Calcd for $C_{74}H_{51}N_9P_2RuZn$ (M_r = 1294.69): C, 68.65; H, 3.97; N, 9.74. Found: C, 67.77; H, 3.78; N, 10.49.

Complex 5. A solution of PPN[Fe(III)Pc(CN)$_2$] (200 mg, 0.17 mmol) and **1b** (94 mg, 0.17 mmol) in methanol (125 mL) was treated with 1 mL of glacial acetic acid and stirred for 3 days. The dark blue precipitate was filtered off, washed with methanol, benzene, and petroleum ether (50 mL each), and dried in vacuo. The residue was taken up in

(28) Atkinson, F. L.; Christofides, A.; Connelly, N. G.; Lawson, H. J.; Loyns, A. C.; Orpen, A. G.; Rosair, G. M.; Worth, G. H. *J. Chem. Soc., Dalton Trans.* **1993**, 1441.
(29) Kalz, W.; Homborg, H. *Z. Naturforsch.* **1983**, *38b*, 470.

Table 3. Crystallographic Data

	3·0.5CH_2Cl_2·THF	**6**·2$CHCl_3$	[**9a**]SbF_6	[**10a**]SbF_6	**8b**·1$^1/_2CH_2Cl_2$	[**10b**]SbF_6
formula	$C_{68.5}H_{54}ClFeN_9OP_2Zn$	$C_{77}H_{53}Cl_6FeN_{10}P_2Ru$	$C_{96}H_{74}F_6Fe_3N_{10}P_4Sb$	$C_{116}H_{86}F_6FeN_{10}P_4Ru_2Sb$	$C_{119}H_{92}Cl_6FeN_{10}P_4Ru_2$	$C_{116}H_{86}F_6FeN_{10}P_4Ru_2Sb$
MW	1237.9	1549.8	1894.8	2237.6	2256.6	2237.6
space group	$P2_1/n$	$P\bar{1}$	$P2_1/n$	$P\bar{1}$	$C2/c$	$P2_1/n$
Z	4	2	2	2	4	4
a (Å)	21.620(4)	13.570(4)	18.935(4)	14.348(3)	25.941(5)	26.902(8)
b (Å)	12.172(2)	15.394(4)	9.017(1)	16.021(3)	25.999(5)	14.788(4)
c (Å)	22.861(5)	18.178(6)	25.538(7)	25.072(5)	17.352(3)	29.957(11)
α (deg)	90	93.98(2)	90	81.22(3)	90	90
β (deg)	94.75(3)	103.32(3)	97.53(2)	81.26(3)	119.50(3)	108.08(2)
γ (deg)	90	106.34(2)	90	79.73(3)	90	90
V (Å^3)	5995(2)	3466(2)	9322(2)	5558(2)	10186(3)	11329(6)
d calcd (g cm^{-3})	1.37	1.49	1.46	1.34	1.47	1.31
μ MoKα (mm^{-1})	0.79	0.76	0.94	0.75	0.71	0.74
R1 (obs. reflns)[a]	0.071	0.075	0.071	0.073	0.057	0.079
wR2 (all reflns)[b]	0.229	0.240	0.250	0.248	0.155	0.266

[a] $R1 = \sum|F_o - F_c|/\sum F_o$. [b] $wR2 = \sum[w(F_o^2 - F_c^2)^2]/\sum[w(F_o^2)]^{1/2}$.

chloroform (70 mL), filtered, and layered carefully with petroleum ether (bp 60−70 °C). Within a few days, 96 mg (49%) of **5** had precipitated as black crystals (mp 260 °C dec).

Anal. Calcd for $C_{65}H_{45}Fe_2N_{10}P_2$ (M_r = 1139.78): C, 68.50; H, 3.98; N, 12.29. Found: C, 67.51; H, 3.96; N, 12.30.

Complex 6. Complex **6** was prepared like **5** but with PPN[Fe(III)Pc(CN)$_2$] (200 mg, 0.17 mmol) and **2b** (124 mg, 0.17 mmol), yielding 115 mg (51%) of black crystals (mp 250 °C dec).

Anal. Calcd for $C_{75}H_{51}FeN_{10}P_2Ru$ (M_r = 1311.16): C, 68.70; H, 3.92; N, 10.68. Found: C, 68.17; H, 3.83; N, 10.86.

Complex 7a. A solution of FePc (200 mg, 0.35 mmol) and **1b** (1.15 g, 2.11 mmol) in toluene (30 mL) was heated and refluxed for 5 h, filtered hot, and then cooled to −30 °C to precipitate excess **1b**. After being filtered, the solution was evaporated to dryness, and the residue was washed with CH_3CN, diethyl ether, and petroleum ether (30 mL each) and then dried in vacuo. It was taken up in benzene (30 mL) and carefully layered with petroleum ether (bp 60−70 °C). Within 1 week, 75 mg (13%) of **7a** had separated as dark green powder (mp 200 °C dec).

Anal. Calcd for $C_{96}H_{74}Fe_3N_{10}P_4$ (M_r = 1659.14): C, 69.50; H, 4.50; N, 8.44. Found: C, 69.51; H, 4.56; N, 8.49.

Complex 8a. Complex **8a** was prepared like **7a** but with FePc (108 mg, 0.19 mmol) and **2b** (817 mg, 1.14 mmol), yielding 113 mg (27%) of **8a**·2CH_2Cl_2 as dark green crystals (mp 245 °C dec).

Anal. Calcd for $C_{118}H_{90}Cl_4FeN_{10}P_4Ru_2$ (M_r = 2171.77): C, 65.26; H, 4.18; N, 6.45. Found: C, 65.53; H, 4.05; N, 6.35.

Complex 7c. This preparation describes one of several similar attempts to obtain pure **7c**. A solution of (PPN)$_2$[Fe(II)Pc(CN)$_2$] (212 mg, 0.12 mmol) and **1a** (150 mg, 0.25 mmol) in methanol (50 mL) was stirred for 5 h. The precipitate was filtered off, washed with methanol (10 mL), diethyl ether (20 mL), and petroleum ether (20 mL), and dried in vacuo to yield 121 mg (58%) of **7c** as black powder (mp 189 °C dec).

Anal. Calcd for $C_{96}H_{74}Fe_3N_{10}P_4$ (M_r = 1659.14): C, 69.50; H, 4.50; N, 8.44. Found: C, 69.51; H, 4.56; N, 8.49.

Complex 8b. Complex **8c** was prepared like **7c** but with (PPN)$_2$[Fe(II)Pc(CN)$_2$] (213 mg, 0.13 mmol) and **2a** (182 mg, 0.25 mmol) in methanol (50 mL). The raw product was taken up in dichloromethane (50 mL) and layered carefully with petroleum ether (bp 60−70 °C). Within a few days, 247 mg (67%) of **8b** had separated as dark green needles (mp 200 °C dec).

Anal. Calcd for $C_{116}H_{86}FeN_{10}P_4Ru_2$ (M_r = 2001.91): C, 69.60; H, 4.33; N, 7.00. Found: C, 68.57; H, 4.28; N, 7.71.

Complex 9a. A suspension of Fe(III)PcCl (148 mg, 0.25 mmol) and **1b** (268 mg, 0.49 mmol) in methanol (100 mL) was stirred for 12 h. After the solution was filtered, 63 mg (0.25 mmol) of $NaSbF_6$ was added, and the solution was filtered again and evaporated to dryness. The residue was taken up in dichloromethane (20 mL) and layered carefully with petroleum ether (bp 60−70 °C). After several days, 176 mg (38%) of [**9a**]SbF_6 had separated as dark blue needles (mp 215 °C dec).

Anal. Calcd for $C_{96}H_{74}F_6Fe_3N_{10}P_4Sb$ (M_r = 1894.88): C, 60.85; H, 3.94; N, 7.39. Found: C, 58.16; H, 3.84; N, 6.49.

Complex 10a. Complex **10a** was prepared like **9a** but with 157 mg (0.26 mmol) of Fe(III)PcCl, 373 mg (0.52 mmol) of **2b**, and 67 mg (0.26 mmol) of $NaSbF_6$. The raw product was analytically pure without recrystallization. The yield of [**10a**]SbF_6 was 171 mg (29%) as black powder (mp 275 °C dec).

Anal. Calcd for $C_{116}H_{86}F_6FeN_{10}P_4Ru_2Sb$ (M_r = 2237.64): C, 62.27; H, 3.87; N, 6.26. Found: C, 61.28; H, 3.71; N, 6.13.

Complex 10b. Complex **10b** was prepared like **10a** but with 200 mg (0.17 mmol) of PPN[Fe(III)Pc(CN)$_2$], 251 mg (0.35 mmol) of **2a**, and 45 mg (0.17 mmol) of $NaSbF_6$. The yield of [**10b**]SbF_6 was 195 mg (51%) as black powder (mp 235 °C dec).

Anal. Calcd for $C_{116}H_{86}F_6FeN_{10}P_4Ru_2Sb$ (M_r = 2237.64): C, 62.27; H, 3.87; N, 6.26. Found: C, 62.19; H, 4.30; N, 6.00.

Alternatively, a solution of **6** (103 mg, 0.08 mmol) and [RuCp(PPh$_3$)$_2$(CH$_3$CN)]SbF_6 (76 mg, 0.08 mmol) in dichloromethane (50 mL) was stirred for 12 h, filtered, and evaporated to dryness. The residue was taken up in dichloromethane (20 mL), filtered, and layered carefully with petroleum ether (bp 60−70 °C). Within a few days, 137 mg (78%) of [**10b**]SbF_6 had separated as black crystals.

Complex 9b. A solution of **5** (105 mg, 0.09 mmol) and [FeCp(dppe)(CH$_3$CN)]SbF_6 (69 mg, 0.09 mmol) in dichloromethane (50 mL) was stirred for 3 h and then subjected to IR and NMR spectroscopy, which showed that the major species in solution was **9b**. Further stirring of the solution for 6 h and workup in the procedure described for **9a** yielded 51 mg (35%) of [**9a**]SbF_6.

Complex 11b. A solution of **5** (105 mg, 0.09 mmol) and [RuCp(PPh$_3$)$_2$(CH$_3$CN)]SbF_6 (89 mg, 0.09 mmol) in dichloromethane (50 mL) was stirred for 12 h, filtered, and evaporated to dryness. The residue was taken up in dichloromethane (20 mL) and layered carefully with petroleum ether (bp 60−70 °C). After a week, 126 mg (66%) of [**11b**]SbF_6 had separated as dark blue needles (mp 230 °C dec).

Anal. Calcd for $C_{106}H_{80}F_6Fe_2N_{10}P_4RuSb$ (M_r = 2066.26): C, 61.62; H, 3.90; N, 6.78. Found: C, 61.51; H, 4.15; N, 6.55.

Complex 12b. Complex **12b** was prepared like **11b** but with **6** (98 mg, 0.07 mmol) and [FeCp(dppe)(CH$_3$CN)]SbF_6 (60 mg, 0.07 mmol). The yield of [**12b**]SbF_6 was 121 mg (78%) as dark blue crystals (mp 215 °C dec).

Anal. Calcd for $C_{106}H_{80}F_6Fe_2N_{10}P_4RuSb$ (M_r = 2066.26): C, 61.62; H, 3.90; N, 6.78. Found: C, 60.79; H, 4.09; N, 5.87.

Complex 9c. A solution of **7c** (100 mg, 0.06 mmol) in dichloromethane (50 mL) was treated dropwise at −70 °C with a solution of [FeCp$_2$]SbF_6 (25 mg, 0.06 mmol) in dichloromethane (10 mL). After the solution was filtered at −70 °C, the solvent was removed in vacuo at −70 °C. The residue was washed three times with toluene at −70 °C and then taken up at −70 °C in dichloromethane (8 mL), filtered, and layered carefully at −70 °C with petroleum ether (bp 60−70 °C). After 2 weeks at −30 °C, 89 mg (78%) of [**9c**]SbF_6 had separated as dark blue needles (mp 165 °C dec). When the spectra were taken at

room temperature, increasing amounts of **9a** in the solution could be detected.

Anal. Calcd for $C_{96}H_{74}F_6Fe_3N_{10}P_4Sb$ (M_r = 1894.88): C, 60.85; H, 3.94; N, 7.39. Found: C, 58.96; H, 3.62; N, 7.22.

Structure Determinations. Crystals were taken from the isolated compounds without further recrystallization. They were sealed in glass capillaries. Diffraction data were taken at 190 K on a Nonius CAD4 diffractometer with graphite-monochromatized MoKα radiation (λ = 0.7107 Å). The structures were solved without an absorption correction by direct methods and refined anisotropically with the SHELX program suite.[30] Hydrogen atoms were included with fixed distances and isotropic temperature factors 1.2 times those of their attached atoms. Parameters were refined against F^2. Drawings were produced with SCHAKAL.[31] Table 3 lists the crystallographic data.

Acknowledgment. This work was supported by the Graduiertenkolleg "Ungepaarte Elektronen" of the Deutsche Forschungsgemeinschaft. The authors thank D. Fenske of Karlsruhe for obtaining three X-ray data sets.

Supporting Information Available: Fully labeled ORTEP plots and X-ray crystallographic files in CIF format for the six structure determinations and graphical representations of the kinetic analysis of the **9c** → **9a** isomerization. This material is available free of charge via the Internet at http://pubs.acs.org.

IC0001412

(30) Sheldrick, G. M. *SHELXS-86 and SHELXL-93*; Universität Göttingen: Göttingen, Germany, 1986 and 1993.

(31) Keller, E. *SCHAKAL for Windows*; Universität Freiburg: Freiburg, Germany, 1999.